Discovery of New Lines in the $R9$ Multiplet of the $2v_3$ Band of $^{12}CH_4$

H. Lin,[1,*,‡] L. Yang,[1,2,‡] X. J. Feng,[1] and J. T. Zhang[1,2,†]
[1]Division of Thermophysics and Process Measurements, National Institute of Metrology, 18 Bei San Huang Dong Lu, Chao Yang District, Beijing 100029, China
[2]Department of Precision Instrument, Tsinghua University, 1 Qing Hua Yuan, Hai Dian District, Beijing 100084, China

(Received 23 October 2018; published 9 January 2019)

We present the first results for resolving methane (CH_4) line transition frequencies down to the kilohertz level for overlapping lines using comb-linked cavity ring-down spectroscopy, while most available laboratory measurements, having resolution at the megahertz level, cannot separate merged lines. To demonstrate the technique, Lamb-dip spectra and linear-absorption spectra were used to identify overlapped lines of vibration-rotation spectra in the $R9$ multiplet of the $2v_3$ band. Three new weak lines were found for the first time. The experimental methods are extensible to other important bands of CH_4 and many other gas-phase molecules, and should provide a more detailed understanding of molecular structure and line parameters for future high-precision studies.

DOI: 10.1103/PhysRevLett.122.013002

Methane (CH_4) is the prototypical saturated hydrocarbon and plays a crucial role in fields such as astrophysics, geosciences, atmospheric and environmental science, reaction dynamics, and combustion science. It is present in many celestial bodies ranging from planetary systems in our Solar System such as those of Jupiter [1] and Saturn [2], to those of distant stars [3,4]. Recently, its presence has been suggested in the atmosphere of Mars [5], raising many questions about its origin. In addition to its importance in planetary studies, the methane molecule is also a tool for basic science, e.g., studies of time-dependent quantum dynamics [6], nine-dimensional calculations of time-independent vibrational quantum eigenstates, and dynamical chirality from *ab initio* calculations [6,7]. In all these fields there is strong interest in the modeling of methane's high-resolution spectrum. Several projects are flying experiments or even whole missions either specifically to monitor the atmospheric CH_4 content or as part of wider scientific programs (e.g., SCIAMACHY [8], GOSAT [9], CARBONSAT [10], SENTINEL 5 [11], MERLIN [12]).

However, due to the high-symmetry of the molecule and the related polyad structure of close lying levels, it is often very difficult to obtain the correct spectral parameters, e.g., for line centers and intensities. The four normal-mode frequencies v_i of CH_4 exhibit an approximate relation of stretching and bending frequencies with $v_1 \approx v_2 \approx 2v_3 \approx 2v_4$. This results in vibrational levels being grouped into polyads with levels of similar energy. However, unlike other small molecules such as CO_2 [13], the number of interacting vibrational levels within each polyad increases rapidly with the polyad number, making the line-by-line assignment analysis increasingly challenging in the near infrared region. Because of the strong overlap of transitions, the absorption spectra of CH_4 are often imperfectly resolved even at low pressures < 1 kPa [9,14] or temperatures down to 80 K [15]. In this Letter, we present a novel approach for determining accurate transition frequencies for CH_4 absorption spectra with hitherto unreported accuracy.

The comb-linked cavity ring-down spectroscopy (CRDS) apparatus, developed from our previous frequency-stabilized cavity ring-down spectrometer [16], is shown in Fig. 1. The ring-down cavity contains two mirrors with nominal transmission loss of 2×10^{-5} giving a high finesse (1.6×10^5). The cavity length is about 145 cm and the nominal free spectral range (FSR) 103.38 MHz. The cavity length is stabilized with respect to an I_2-frequency-stabilized He-Ne laser of relative uncertainty of 1.4×10^{-11} (for a 1 s averaging time) [17]. An extended-cavity diode laser (ECDL, Sacher LION) with a wavelength range from 1.55 to 1.63 μm is frequency locked to a resonant frequency of the ring-down cavity by counting the number of ring down events [18]. When the light energy transmitted through the cavity triggers the threshold, the probe laser is switched off by the booster optical amplifier (BOA, Thorlabs BOA1082P) and a 16-bit analog-to-digital converter (ADC, Gage CSE1622) records the ring-down (decay) optical signals [19]. The absorption coefficient α is given by

$$\alpha = \frac{1}{c\tau} = \frac{1}{c\tau_c} + \frac{1}{c\tau_g}, \tag{1}$$

where c is the speed of light, τ the exponential decay time of a ring-down signal, τ_c the decay time of empty cavity, and τ_g the absorption coefficient of simple gases. All the optical frequency devices are linked to an optical frequency

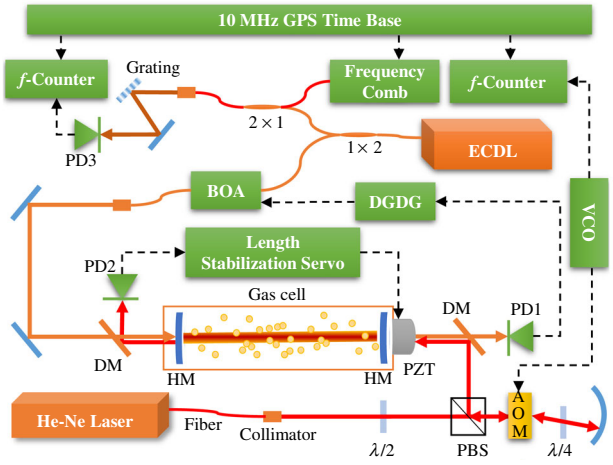

FIG. 1. Experimental apparatus. Extended cavity diode laser (ECDL), booster optical amplifier (BOA), digital gate and delay generator for ring-down signal (DGDG), voltage-controlled oscillator (VCO), high reflectivity mirror (HM), photodetector for measuring ring-down signal (PD1), photodetector for cavity length stabilization (PD2), dichroic mirror (DM), piezo-electric transducer (PZT), Polarization beam splitter (PBS), acoustic-optic modulator (AOM).

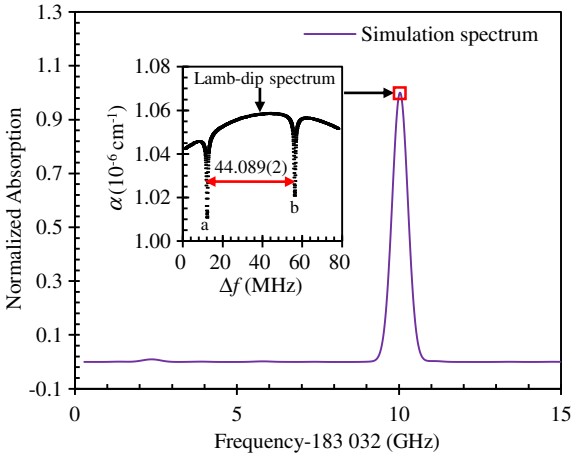

FIG. 2. The two clearly observed Lamb dips of the $10F2 \leftarrow 9F1$ 1(a) and $10F1 \leftarrow 9F2$ 1(b) transitions. We assume the frequency of the $10F1 \leftarrow 9F2$ 1 line is greater than that of $10F2 \leftarrow 9F1$ 1.

comb (OFC, Menlo Systems FC1500-250-WG) traceable to the 10 MHz GPS time base of relative uncertainty of 1×10^{-11}. The first and last spectral points of each spectrum are calibrated by the optical frequency comb.

To measure Lamb-dip spectra, the cavity length is finely scanned using the voltage-controlled oscillator (VCO) [20,21]. The probe laser frequency f_p is locked to a resonant frequency of the cavity and scanned along with the frequency variation Δf_{VCO} of the VCO. Concretely, the Lamb-dip spectral scanning step Δf_p is

$$\Delta f_p = \frac{2f_p}{f_{\mathrm{HeNe}}} \Delta f_{\mathrm{VCO}}, \tag{2}$$

where f_{HeNe} is the He-Ne laser frequency. The spectral scanning step is ≈40 kHz, calibrated by measuring the modulation frequency of the VCO with a frequency counter.

To measure linear-absorption spectra, the probe laser frequency f_p sequentially scanned resonant frequencies of the cavity as discussed in Refs. [16–19] while the modulation frequency of the VCO was constant. In this case, the linear spectral scanning step is the free-spectral range.

We selected the strong overlapped region of the $2v_3$ band $R9$ multiplet of CH_4 as the object of the experiment with which to confront HITRAN, the long-standing database compiled from available high-precision results since the 1960s. The 2012 [22] and 2016 [23] HITRAN versions give 53 and 43 transitions, respectively, with a cutoff line intensity $< 1 \times 10^{-25}$ cm^{-1}/molecule in the region considered here. Such significant differences of transition number and position point to unanswered questions concerning methane spectra.

For example, according to HITRAN2012 [22], the frequencies of the $10F1 \leftarrow 9F2$ 1 and $10F2 \leftarrow 9F1$ 1 transitions are both equal to 183 042 033 MHz, yet according to HITRAN2016 [23] they differ. Table I lists the methane position results from recent papers on linear-absorption spectroscopy. There is obviously serious disagreement between them. We note that all the frequency axes except that of Zolot *et al.* [24] were calibrated using

TABLE I. Some recent results for positions of the overlapped transitions of $10F2 \leftarrow 9F1$ 1 and $10F1 \leftarrow 9F2$ 1 obtained by various authors.

	Transition frequency (MHz)	
Reference	$10F2 \leftarrow 9F1$ 1	$10F1 \leftarrow 9F2$ 1
GOSAT2009 [14]	183 042 056(-)	183 042 056(-)
GOSAT2014 [9]	183 042 035(-)	183 042 056(-)
HITRAN2012 [22]	183 042 033(300)	183 042 033(300)
HITRAN2016 [23]	183 042 035(300)	183 042 056(300)
Zolot *et al.* [24]	183 042 033(450)	183 042 033(450)
Devi *et al.* [27]	183 042 026.882(60)	183 042 039.953(60)
This work	183 042 012.473 1(56)	183 042 056.570 2(49)

TABLE II. The main uncertainty sources of the absolute frequency measurement of the $10F2 \leftarrow 9F1$ 1 transition.

Uncertainty source	Value (kHz)
Statistical uncertainty	5.2
Shift of the GPS time base	1.8
Pressure measurements	0.8
Spectral asymmetry	0.4
Power shift	0.3

TABLE III. Transition frequencies of strong lines of the $2\nu_3$ band $R9$ multiplet of $^{12}CH_4$. The uncertainty of the HITRAN2016 frequencies is 300 MHz for every line.

Transition	$f_{\text{This work}}$ (kHz)	$u(f_{\text{This work}})$ (kHz)	$f_{\text{HITRAN2016}}$ (MHz) [23]
$10F2 \leftarrow 9F1$ 1	183 042 012 473.1	5.6	183 042 056
$10F1 \leftarrow 9F2$ 1	183 042 056 570.2	4.9	183 042 056
—	183 053 069 733.5	4.6	183 053 086
$10E \leftarrow 9E$ 1	183 054 371 570.1	6.2	183 054 341
$10F2 \leftarrow 9F1$ 2	183 054 560 306.9	7.4	183 054 649
$10A2 \leftarrow 9A1$ 1	183 054 789 482.2	3.8	183 054 896
$5F2 \leftarrow 4F1$ 1	183 059 060 207.2	4.1	183 059 064
$10F2 \leftarrow 9F1$ 3	183 059 850 657.7	3.7	183 059 861
$10F1 \leftarrow 9F2$ 2	183 060 789 945.0	3.4	183 060 805
$10A1 \leftarrow 9A2$ 1	183 061 756 287.2	7.4	183 061 763
$5F1 \leftarrow 4F2$ 1	183 088 249 325.2	3.8	183 088 267

HITRAN2008 [25] which retained methane frequencies in the $2\nu_3$ band from a study performed in the late 1980s [26]. Devi *et al.* [27] calibrated their frequency axis using the results of Zolot *et al.* [24] and HITRAN2012 [22]. None of these results can determine positions of the two lines with a satisfactory level of uncertainty.

To investigate this hyperfine spectral structure feature of methane, we used a pure methane gas sample at 0.1(2) Pa and 293.15(5) K to search for Lamb dips of the two transitions near 183 042 033 MHz. The frequency was stepped by 47.4(5) kHz by finely scanning the cavity length. The inset in Fig. 2 clearly shows the two Lamb dips of the rovibrational transitions of $10F2 \leftarrow 9F1$ 1 and $10F1 \leftarrow 9F2$ 1 separated by 44.089(2) MHz. The absorption coefficients at the centers of the two transitions decrease markedly, by about 4%, due to their large Einstein A coefficients (0.92 s^{-1} of $10F1 \leftarrow 9F2$ 1 and 0.85 s^{-1} of $10F2 \leftarrow 9F1$ 1) [23].

We carried out repeated measurements of the Lamb dip of each transition. For $10F2 \leftarrow 9F1$ 1, the absolute frequency was determined to be 183 042 012 473.6 kHz with an overall uncertainty of 5.6 kHz from 24 measurements. The main sources of uncertainty are listed in Table II. Among them, the uncertainty induced by pressure measurements is calculated using the air-pressure shifting coefficient from Devi *et al.* [27]. All uncertainty sources are considered statistically independent. This experimental method was subsequently extended to measurements of the eleven strong transitions in the $2\nu_3$ band R9 multiplet of CH_4. Accurate transition frequencies are listed in Table III.

Lamb-dip spectroscopy only works well for strong transitions. It is extremely difficult to use it alone to determine positions of weak transitions accurately in cases of strong overlap. To solve this problem, therefore, we fitted linear-absorption spectra using fixed strong line positions, already obtained reliably by Lamb-dip spectroscopy. To test this approach, we recorded the linear-absorption spectrum of 498.3 ppm CH_4 (buffered by N_2) at a pressure of 166(1) Pa. At such a pressure, the linear absorption profile of a transition is dominated by the Doppler and molecular collisional broadening effects, well modeled by a Voigt profile with five parameters (ω_0, Γ_D, Γ_0, Δ_0, A) [28]. The Doppler broadening widths Γ_D were fixed at their theoretical values for the actively controlled cell temperature of $T = 296.00(5)$ K. The collisional broadening, Γ_0, and shift, Δ_0, coefficients were fixed at 17.8 and −3.55 kHz/Pa [27], respectively. The only floated parameters were the areas A and the line positions ω_0.

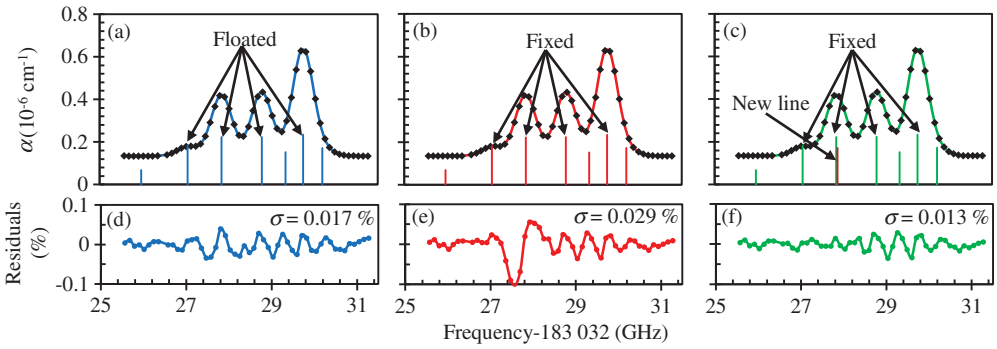

FIG. 3. The fitting comparison of the linear spectrum with different methods: (a) all line positions floated; (b) strong line positions fixed using Lamb-dip results, weak lines floated; (c) like (b) but with an extra weak line added—flatter residuals suggest the existence of a previously unreported line. The symbol σ denotes the standard deviation of the fitting residuals.

To show how this idea works, we compare three different fitting methods in Fig. 3. Case I: all line positions are free. Almost flat fitting residuals were obtained by adding three weak lines [blue vertical lines in Fig. 3(a)]. Case II: the positions of the four strong lines obtained by Lamb-dip spectroscopy were fixed while the three weak line positions were floated. A large deviation near 183 059 863 MHz is apparent in the fitting residuals [Fig. 3(e)]. Case III: based on Case II, we added an extra floating line near 183 059 863 MHz. In this case, the fitting residuals become almost flat [Fig. 3(f)], the maximum relative fitting residuals being 0.04% with respect to the peak absorption. This indicates the existence of a hitherto unreported weak line of 183 059 862.5 MHz with a fitting uncertainty of 2.0 MHz, which would have remained undetected without the help of accurate position information provided by Lamb-dip spectroscopy.

In total, we have measured the frequencies of 56 transitions in the region considered for intensities $>1\times10^{-25}$ cm^{-1}/molecule. Among them, 53 lines are consistent with those given by the HITRAN2012 database. Three new lines of 183 059 862.5(2.0), 183 063 581(50), and 183 057 963(72) MHz were found and determined in this experiment.

The authors acknowledge the financial support by the National Key R&D Program of China (2016YFF0200101) and the Program of International Science & Technology Cooperation of China (2015DFG71880). We would like to thank Dr. J. T. Hodges of NIST and Dr. M. D. Plimmer of LCM-LNE-Cnam for their help on this work.

*Corresponding author.
linhong@nim.ac.cn
†Corresponding author.
zhangjint@nim.ac.cn
‡These authors contributed equally to this work

[1] P. Irwin, K. Sihra, N. Bowles, F. Taylor, and S. Calcutt, Icarus **176**, 255 (2005).
[2] H. Tran, P.-M. Flaud, T. Fouchet, T. Gabard, and J.-M. Hartmann, J. Quant. Spectrosc. Radiat. Transfer **101**, 306 (2006).
[3] J. A. Stansberry, J. R. Spencer, B. Schmitt, A.-I. Benchkoura, R. V. Yelle, and J. I. Lunine, Planet. Space Sci. **44**, 1051 (1996).
[4] E. Lellouch, B. Sicardy, C. de Bergh, H.-U. Käufl, A. Kassi, and S. Campargue, Astron. Astrophys. **495**, L17 (2009).
[5] V. Formisano, S. Atreya, T. Encrenaz, N. Ignatiev, and M. Giuranna, Science **306**, 1758 (2004).
[6] R. Marquardt, M. Quack, and I. Thanopulos, J. Phys. Chem. A **104**, 6129 (2000).
[7] H. Hollenstein, R. R. Marquardt, M. Quack, and M. A. Suhm, J. Chem. Phys. **101**, 3588 (1994).
[8] C. Frankenberg, I. Aben, P. Bergamaschi, E. J. Dlugokencky, R. van Hees, S. Houweling, P. van der Meer, R. Snel, and P. Tol, J. Geophys. Res. **116**, D04302 (2011).
[9] A. V. Nikitin, O. M. Lyulin, S. N. Mikhailenko, V. I. Perevalov, N. N. Filippov, I. M. Grigoriev, I. Morino, Y. Yoshida, and T. Matsunaga, J. Quant. Spectrosc. Radiat. Transfer **154**, 63 (2015).
[10] M. Buchwitz, M. Reuter, H. Bovensmann, D. Pillai, J. Heymann, O. Schneising, V. Rozanov, T. Krings, J. P. Burrows, H. Boesch *et al.*, Atmos. Meas. Technol. **6**, 3477 (2013).
[11] A. Butz, A. Galli, O. Hasekamp, J. Landgraf, P. Tol, and I. Aben, Remote Sens. Environ. **120**, 267 (2012).
[12] C. Stephan, M. Alpers, B. Millet, G. Ehret, P. Flamant, and C. Deniel, *Proceedings of SPIE 8159, Lidar Remote Sensing for Environmental Monitoring XII* (Society of Photo-Optical Instrumentation Engineers (SPIE), Bellingham, Washington, USA, 2011), p. 815908.
[13] O. L. Polyansky, K. Bielska, M. Ghysels, L. Lodi, N. F. Zobov, J. T. Hodges, and J. Tennyson, Phys. Rev. Lett. **114**, 243001 (2015).
[14] A. V. Nikitin, O. M. Lyulin, S. N. Mikhailenko, V. I. Perevalov, N. N. Filippov, I. M. Grigoriev, I. Morino, T. Yokota, R. Kumazawa, and T. Watanabe, J. Quant. Spectrosc. Radiat. Transfer **111**, 2211 (2010).
[15] A. Campargue, O. Leshchishina, L. Wang, D. Mondelain, S. Kassi, and A. V. Nikitin, J. Quant. Spectrosc. Radiat. Transfer **113**, 1855 (2012).
[16] L. Yang, H. Lin, M. Plimmer, X. Feng, and J. Zhang, J. Quant. Spectrosc. Radiat. Transfer **210**, 82 (2018).
[17] J. T. Hodges, H. P. Layer, W. W. Miller, and G. E. Scace, Rev. Sci. Instrum. **75**, 849 (2004).
[18] J. T. Hodges and R. Ciuryło, Rev. Sci. Instrum. **76**, 023112 (2005).
[19] H. Lin, Z. D. Reed, V. T. Sironneau, and J. T. Hodges, J. Quant. Spectrosc. Radiat. Transfer **161**, 11 (2015).
[20] D. Lisak, J. T. Hodges, and R. Ciuryło, Phys. Rev. A **73**, 012507 (2006).
[21] D. Lisak and J. T. Hodges, Appl. Phys. B **88**, 317 (2007).
[22] L. Rothman, I. Gordon, Y. Babikov, A. Barbe, D. C. Benner, P. Bernath, M. Birk, L. Bizzocchi, V. Boudon, L. Brown *et al.*, J. Quant. Spectrosc. Radiat. Transfer **130**, 4 (2013), HITRAN2012 special issue.
[23] I. E. Gordon, L. S. Rothman, C. Hill, R. V. Kochanov, Y. Tan, P. F. Bernath, M. Birk, V. Boudon, A. Campargue, K. V. Chance *et al.*, J. Quant. Spectrosc. Radiat. Transfer **203**, 3 (2017).
[24] A. M. Zolot, F. R. Giorgetta, E. Baumann, W. C. Swann, I. Coddington, and N. R. Newbury, J. Quant. Spectrosc. Radiat. Transfer **118**, 26 (2013).
[25] L. Rothman, I. Gordon, A. Barbe, D. Benner, P. Bernath, M. Birk, V. Boudon, L. Brown, A. Campargue, J.-P. Champion *et al.*, J. Quant. Spectrosc. Radiat. Transfer **110**, 533 (2009).
[26] J. S. Margolis, Appl. Opt. **27**, 4038 (1988).
[27] V. M. Devi, D. C. Benner, K. Sung, T. J. Crawford, S. Yu, L. R. Brown, M. A. H. Smith, A. W. Mantz, V. Boudon, and S. Ismail, J. Mol. Spectrosc. **315**, 114 (2015).
[28] N. H. Ngo, D. Lisak, H. Tran, and J.-M. Hartmann, J. Quant. Spectrosc. Radiat. Transfer **129**, 89 (2013).